Wang et al. *EPJ Quantum Technology* (2021) 8:21
https://doi.org/10.1140/epjqt/s40507-021-00110-1

EPJ Quantum Technology
a SpringerOpen Journal

RESEARCH Open Access

Phase sensitivity of an SU(1, 1) interferometer via product detection

Qingle Wang[1,2], Yami Fang[3,4*], Xiaoping Ma[5] and Dong Li[6,7]

*Correspondence:
fangyami@163.com
[3]Shanghai Aerospace Control Technology Institute, 201109 Shanghai, China
[4]Shanghai Key Laboratory of Aerospace Intelligent Control Technology, 201109 Shanghai, China
Full list of author information is available at the end of the article

Abstract

We theoretically analyze the phase sensitivity of an SU(1, 1) interferometer with various input states by product detection in this paper. This interferometer consists of two parametric amplifiers that play the role of beam splitters in a traditional Mach–Zehnder interferometer. The product of the amplitude quadrature of one output mode and the momentum quadrature of the other output mode is measured via balanced homodyne detection. We show that product detection has the same phase sensitivity as parity detection for most cases, and it is even better in the case with two coherent states at the input ports. The phase sensitivity is also compared with the Heisenberg limit and the quantum Cramér–Rao bound of the SU(1, 1) interferometer. This detection scheme can be easily implemented with current homodyne technology, which makes it highly feasible. It can be widely applied in the field of quantum metrology.

Keywords: Phase sensitivity; SU(1, 1) interferometer; Product detection

1 Introduction

Quantum parameter estimation has recently drawn considerable attention for its fundamental and technological applications [1–12]. One of the most common and powerful tools in the field of precision metrology is optical interferometry, because of its extreme phase sensitivity. However, the phase sensitivity $\Delta\phi$ of an interferometer with solely classical resources is bounded by $1/\sqrt{\bar{n}}$, which is well known as the shot noise limit (SNL), where $\bar{n}$ is the average photon number. During the past few decades, it has been shown that this limit can be surpassed by taking advantage of quantum resources. By using particle entanglement as a resource for sensitivity enhancement [13, 14], there has been much progress toward reaching the more fundamental Heisenberg limit (HL), which is characterized by a phase sensitivity scale of $1/\bar{n}$.

One possibility for beating the SNL is to inject non-classical light into a traditional interferometer, such as a Mach–Zehnder interferometer. A number of theoretical proposals have shown that the phase sensitivity can go below the SNL using non-classical light, such as squeezed states [15, 16], two-mode squeezed states [17], Fock states [18] and NOON states [19–21].

Another possibility for beating the SNL is to use a new class of interferometers, which is described by the SU(1, 1) group, unlike the Mach–Zehnder interferometer by the SU(2) group. This type of interferometer, which was first proposed by Yurke *et al.* [22], is shown in Fig. 1. It is configured as a Mach–Zehnder interferometer, except that the beam splitters are replaced by parametric amplifiers (PAs), such as optical parametric amplifiers or four-wave mixers. It has been pointed out that a phase sensitivity with vacuum inputs scaling as $1/[\bar{n}(\bar{n}+2)]^{1/2}$ can be achieved with intensity detection, where $\bar{n} = 2\sinh^2 g$ is the average photon number inside the interferometer and g is the PA interaction strength. Although the phase sensitivity reaches the HL, $\bar{n}$ is small due to the limited interaction strength g.

Recently, a new theoretical scheme utilizing coherent states as inputs showed that the phase sensitivity can be largely enhanced in the interferometer as a result of the large input photon number [23]. Marino *et al.* [24] also studied the effect of loss on the phase sensitivity of the SU(1, 1) interferometer with intensity detection. Sparaciari *et al.* [25, 26] analyzed the phase sensitivity in SU(1, 1) interferometers initially fed by Gaussian states. It is found that incident coherent states could lead to Heisenberg scaling. Hu *et al.* [27] investigated the effect of phase diffusion on the performance of an SU(1, 1) interferometer. You *et al.* [28] revisited the phase sensitivity in an SU(1, 1) interferometer considering the different phase configurations. More recently, Zhang *et al.* [29] addressed the quantum stochastic phase estimation with SU(1, 1) interferometer.

Experimental realizations of the SU(1, 1) interferometer have been reported in optical systems [30, 31], spinor Bose–Einstein condensates (BECs) [32–36], a hybrid atom-light interferometer [37, 38], and a circuit quantum electrodynamics system [39]. Most recently, an alternative "pumped-up" approach was proposed [40] where all the particles can be involved in the quantum parameter estimation. It can be implemented in spinor BECs and hybrid atom-light systems. In this manuscript, we consider the SU(1, 1) interferometer which is realized in optical system.

One goal of precision metrology is to achieve the HL. For this purpose, several different detection schemes have also been thoroughly investigated, including intensity detection [23], homodyne detection [41] and parity detection [42]. It has been pointed out that an SU(1, 1) interferometer with coherent and squeezed vacuum states as inputs can approach the HL with both homodyne and parity detection. Another kind of scheme, product detection, which was first proposed in Ref. [17], can achieve the HL scaling with two-mode squeeze states as inputs in a traditional Mach–Zehnder interferometer. Mathematically, product detection is described by $\hat{P} = (\hat{a} + \hat{a}^\dagger)(\hat{b} - \hat{b}^\dagger)/2i$, where $\hat{a}$ ($\hat{a}^\dagger$) and $\hat{b}$ ($\hat{b}^\dagger$) are the annihilation (creation) operators for the two output modes. We adjust the relative phases of the local oscillators in homodyne detection such that the photocurrents of detectors a and b are proportional to the expectation values of the amplitude quadrature $(\hat{a} + \hat{a}^\dagger)/\sqrt{2}$ and the momentum quadrature $(\hat{b} - \hat{b}^\dagger)/\sqrt{2}i$. In this way, product detection can be easily implemented by homodyne technique. Compared with parity detection, product detection does not require a photon-number resolving detector, which makes it much more feasible.

In this paper, we consider a single-mode squeezed state $|\psi\rangle = \hat{D}(\alpha)\hat{S}(r)|0\rangle$ as input, where $\hat{S}(r) = e^{(r^*\hat{a}^2 - r\hat{a}^{\dagger 2})/2}$ is the squeezing operator, $\hat{D}(\alpha) = e^{(\alpha\hat{a}^\dagger - \alpha^*\hat{a})}$ is the displacement operator [43], $r = |r|e^{i\phi_r}$ is the squeezing parameter, $\alpha = |\alpha|e^{i\theta_a}$ is the displacement amplitude, and r^* and α^* are the conjugate of r and α, respectively. Specifically, when $r = 0$, it reduces to a coherent state, and when $\alpha = 0$, it is a squeezed vacuum state. Using this

method, we can easily go back to some specific inputs, such as a coherent state mixed with squeezed vacuum state [41, 42]. We show that with the coherent state and the squeezed vacuum state as inputs, the phase sensitivity with product detection can approach the HL (as in Ref. [42]) when the average photon number of the coherent and squeezed vacuum states are comparable. Furthermore, we discuss the condition for achieving the optimal phase sensitivity with different input states. Finally, we also compare the phase sensitivity with another quantum limit, the quantum Cramér–Rao bound (QCRB) [44], which quantifies the ultimate limit on the performance of the phase-estimation strategies for a given quantum state.

This paper is organized as follows: We first present the propagation of the input fields through the SU(1, 1) interferometer in Sect. 2. We then discuss the HL in an SU(1, 1) interferometer and compare the phase sensitivity with the HL and the QCRB in Sect. 3. After comparing different detection schemes in Sect. 4, we conclude with a summary.

2 Product detection on SU(1, 1) interferometer

2.1 Model

Figure 1 shows the model of an SU(1, 1) interferometer, in which two PAs play the role of beam splitters in a traditional Mach–Zehnder interferometer. We consider single-mode squeezed states as inputs. $\hat{a}$ ($\hat{a}^\dagger$) and $\hat{b}$ ($\hat{b}^\dagger$) are the annihilation (creation) operators corresponding to the modes a and b, respectively. After the first PA, one output beam accumulates a phase shift ϕ. The output beams are measured via homodyne detection. The phase information can be inferred from the measured signal.

This interferometer can be modeled by the transformation between input and output modes by $\hat{V}_2 = T_2 T_\phi T_1 \hat{V}_0$, where $\hat{V}_2 = (\hat{a}_2, \hat{a}_2^\dagger, \hat{b}_2, \hat{b}_2^\dagger)^T$ and $\hat{V}_0 = (\hat{a}_0, \hat{a}_0^\dagger, \hat{b}_0, \hat{b}_0^\dagger)^T$. T_1, T_ϕ, and T_2 describe the first PA, the phase shift and the second PA, respectively:

$$T_1 = \begin{pmatrix} \mu_1 & 0 & 0 & \nu_1 \\ 0 & \mu_1 & \nu_1^* & 0 \\ 0 & \nu_1 & \mu_1 & 0 \\ \nu_1^* & 0 & 0 & \mu_1 \end{pmatrix}, \tag{1}$$

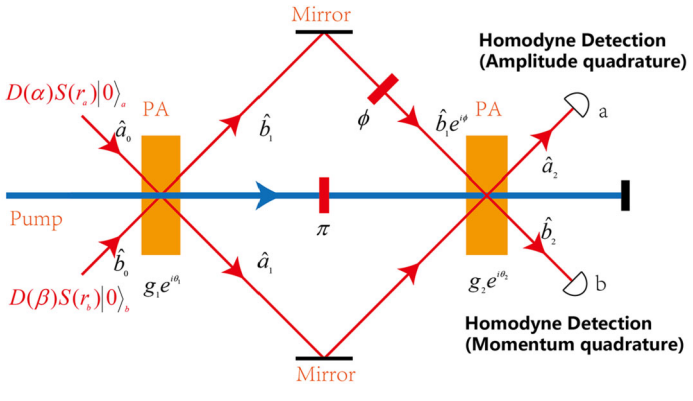

Figure 1 (Color online) Schematic diagram of SU(1, 1) interferometer. Two parametric amplifiers (PAs) take the place of two beam splitters in the traditional Mach–Zehnder interferometer. g_1 (g_2) and θ_1 (θ_2) describe the strength and phase shift introduced by the parametric processes, respectively. $\hat{a}_i$ and $\hat{b}_i$ ($i = 0, 1, 2$) denote two modes in the different processes. The pump field between the two PAs has a π phase difference

$$T_\phi = \begin{pmatrix} 1 & 0 & 0 & 0 \\ 0 & 1 & 0 & 0 \\ 0 & 0 & e^{i\phi} & 0 \\ 0 & 0 & 0 & e^{-i\phi} \end{pmatrix}, \tag{2}$$

$$T_2 = \begin{pmatrix} \mu_2 & 0 & 0 & \nu_2 \\ 0 & \mu_2 & \nu_2^* & 0 \\ 0 & \nu_2 & \mu_2 & 0 \\ \nu_2^* & 0 & 0 & \mu_2 \end{pmatrix}, \tag{3}$$

where $\mu_j = \cosh g_j$, $\nu_j = -e^{i\theta_j} \sinh g_j$, g_j and θ_j are the strength and phase shift introduced by the PA process j ($j = 1, 2$) [45, 46]. The phase sensitivity of this device by product detection can be obtained through an error propagation analysis,

$$\Delta\phi = \frac{\langle \Delta \hat{P} \rangle}{|\partial \langle \hat{P} \rangle / \partial \phi|}, \tag{4}$$

where the brackets denote the quantum mechanical expectation values, the product operator is defined as $\hat{P} \equiv (\hat{a}_2 + \hat{a}_2^\dagger)(\hat{b}_2 - \hat{b}_2^\dagger)/2i$, and $\langle \Delta \hat{P} \rangle \equiv \sqrt{\langle \hat{P}^2 \rangle - \langle \hat{P} \rangle^2}$ is the standard deviation of the product operator. Usually, the SU(1, 1) interferometer is operated in a balanced configuration in which the second PA will "undo" what the first one does [24]. In such a case, we have $\theta_1 = 0$, $\theta_2 = \pi$, and $g_1 = g_2 = g$. Thus if $\phi = 0$, then $\hat{a}_2 = \hat{a}_0$ and $\hat{b}_2 = \hat{b}_0$. We will focus on a balanced configuration throughout this paper. The input states can be generally expressed by $\hat{D}(\alpha)\hat{S}(r_a)|0\rangle_a \otimes \hat{D}(\beta)\hat{S}(r_b)|0\rangle_b$, where $\alpha = |\alpha| e^{i\theta_a}$, $\beta = |\beta| e^{i\theta_b}$, $r_a = r_1 e^{i\phi_1}$, and $r_b = r_2 e^{i\phi_2}$. Various input states can be obtained from this generality.

2.2 Phase sensitivity

Product detection was firstly proposed in Ref. [17]. It can approach the HL scaling. Here we will study the phase sensitivity with various input states and compare them with the corresponding HL and QCRB.

The corresponding HL [24] is related to the total average photon number inside the interferometer $N_{\text{total}} = \langle \hat{a}_1^\dagger \hat{a}_1 + \hat{b}_1^\dagger \hat{b}_1 \rangle$, which is given by

$$\begin{aligned} N_{\text{total}} = {} & (N_{\text{PA}} + 1)(N_a + N_b + N_{\text{sa}} + N_{\text{sb}}) + N_{\text{PA}} \\ & - 2\sqrt{N_{\text{PA}}(N_{\text{PA}} + 2)}\sqrt{N_a N_b}\cos(\theta_a + \theta_b), \end{aligned} \tag{5}$$

where $N_{\text{PA}} = 2\sinh^2 g$, $N_a = |\alpha|^2$, $N_b = |\beta|^2$, and $N_{\text{s(a,b)}} = \sinh^2 r_{(1,2)}$. Thus, N_{total} not only depends on the strength of the process g, but also on the phase of the input states θ_a and θ_b [46]. Thus, the HL is as follows:

$$\Delta\phi_{\text{HL}} = \frac{1}{N_{\text{total}}}. \tag{6}$$

2.2.1 Vacuum input states $|0\rangle_a \otimes |0\rangle_b$

With vacuum inputs, the optimal phase sensitivity is found to be $\Delta\phi_{\text{opt}} = 1/\sqrt{N_{\text{PA}}(N_{\text{PA}} + 2)}$, while the corresponding HL is $\Delta\phi_{\text{HL}} = 1/N_{\text{PA}}$. The QCRB in this case is also $1/\sqrt{N_{\text{PA}}(N_{\text{PA}} + 2)}$ [42]. Figure 2 compares the phase sensitivity $\Delta\phi_{\text{V}}$ with the SNL,

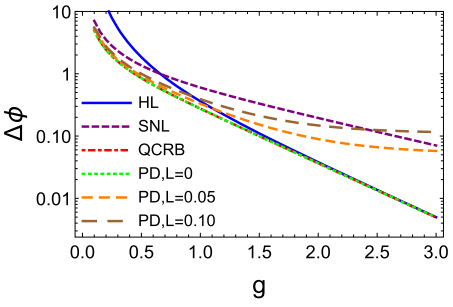

Figure 2 (Color online) Optimal phase sensitivity via product detection as a function of g with a vacuum as inputs. The blue line represents the HL, the dashed purple line represents the shot noise limit (SNL), the dot-dashed red line represents the quantum Cramér–Rao bound (QCRB), the dotted green line represents the phase sensitivity via product detection in the ideal case, the dashed red line represents the phase sensitivity via product detection with photon loss $L = 0.05$, and the dashed brown line represents the phase sensitivity via product detection with photon loss $L = 0.10$

HL, and QCRB, as functions of g. We assume that the interferometer is seeded with pure Gaussian states throughout the paper. As g increases, the phase sensitivity $\Delta\phi$ becomes closer to the HL and it can saturate the QCRB. As shown in Ref. [42], intensity detection, homodyne detection, and parity detection can saturate the QCRB as well. From an experimental perspective, intensity detection is much more preferred in this case.

2.2.2 One coherent input state $|\alpha\rangle_a \otimes |0\rangle_b$

With only one coherent state at the input ports, the first PA works as a phase insensitive amplifier. The phase sensitivity with product detection at $\phi = 0$ is given by

$$\Delta\phi = \sqrt{\frac{1 + 2N_a + 2N_a\cos 2\theta_a}{\kappa(1 + N_a + N_a\cos 2\theta_a)^2}}, \tag{7}$$

where $\kappa = N_{\mathrm{PA}}(N_{\mathrm{PA}} + 2)$. The optimal phase sensitivity is obtained at $\theta_a = 0$. When $N_a \gg 1$, the optimal phase sensitivity can be simplified to

$$\Delta\phi_{\mathrm{opt}} \simeq \frac{1}{\sqrt{\kappa(N_a + 1)}}. \tag{8}$$

This agrees with the parity detection result [42]. Both detection schemes cannot saturate the QCRB. The corresponding HL is $\Delta\phi_{\mathrm{HL}} = 1/[(N_{\mathrm{PA}} + 1)N_a + N_{\mathrm{PA}}]$. The QCRB can be found as $1/[\kappa(2N_a + 1) + 2N_a(N_{\mathrm{PA}} + 2)]^{1/2}$ in Ref. [42]. As shown in Fig. 3, the optimal phase sensitivity can beat the SNL, but it does not surpass the HL. With the increase in g, the phase sensitivity via product detection becomes closer to the QCRB, as shown in Fig. 3(a). As N_a increases, the phase sensitivity can be approximated as $1/\sqrt{N_{\mathrm{PA}}N_{\mathrm{total}}}$. It is improved by a factor of $1/\sqrt{N_{\mathrm{PA}}}$ compared with the SNL as shown in Fig. 3(b). The enhancement arises from the amplification of the parametric process.

2.2.3 Two coherent input states $|\alpha\rangle_a \otimes |\beta\rangle_b$

With two coherent states at the input ports, the first PA works as a phase sensitive amplifier. The amplification will depend on the relative phase between the two input beams. For simplicity, here we assume that two coherent input states have the same photon number, $N_a = N_b$. The phase sensitivity at $\phi = 0$ is obtained by

$$\begin{aligned}\Delta\phi = {} & \sqrt{1 + 4N_a + 2N_a(\cos 2\theta_a - \cos 2\theta_b)} \\ & \times \left[4N_a\left(\sin\theta_a \sin\theta_b \sinh^2 g - \cos\theta_a \cos\theta_b \cosh^2 g\right)\right. \\ & \left. + N_a(2 + \cos 2\theta_a - \cos 2\theta_b)\sinh 2g + \sinh 2g\right]^{-1}.\end{aligned} \tag{9}$$

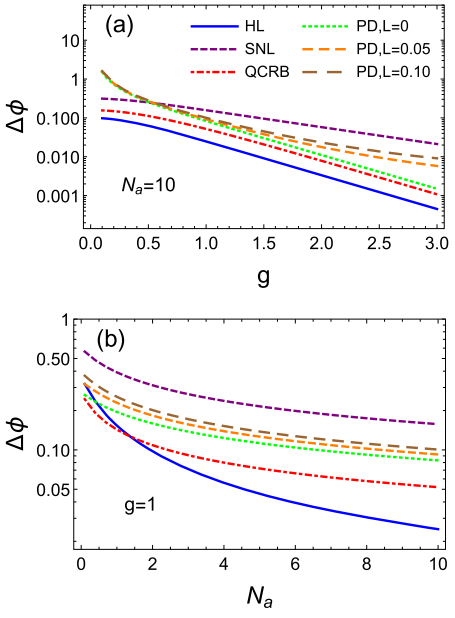

Figure 3 (Color online) Optimal phase sensitivity via product detection as a function of (**a**) g and (**b**) N_a with one coherent input state. The blue line represents the HL, the dashed purple line represents the shot noise limit (SNL), the dot-dashed red line represents the quantum Cramér–Rao bound (QCRB), the dotted green line represents the phase sensitivity via product detection in the ideal case, the dashed red line represents the phase sensitivity via product detection with photon loss $L = 0.05$, and the dashed brown line represents the phase sensitivity via product detection with photon loss $L = 0.10$

Under the condition $\theta_a = 0$ and $\theta_b = \pi$, the optimal phase sensitivity is achieved (here we assume that $N_a \gg 1$):

$$\Delta\phi_{\text{opt}} \simeq \left\{2N_a\left[(N_{\text{PA}}+2)(\sqrt{\kappa}+1)+\kappa\right]+\kappa\right\}^{-1/2}. \tag{10}$$

The corresponding HL is given by

$$\Delta\phi_{\text{HL}} = \frac{1}{2N_a(N_{\text{PA}}+1+\sqrt{\kappa})+N_{\text{PA}}}. \tag{11}$$

According to the general formalism for the QCRB of Gaussian states by Gao *et al.* [47], $\Delta\phi_{\text{QCRB}}$ is given by

$$\Delta\phi_{\text{QCRB}} = \left\{\kappa+4N_a\left[\kappa+1+\sqrt{\kappa}(N_{\text{PA}}+1)\right]\right\}^{-1/2}. \tag{12}$$

Figure 4 shows that the optimal phase sensitivity can beat the SNL, but not the HL, and it is very close to the QRCB.

2.2.4 Coherent state mixed with squeezed vacuum state $|\alpha\rangle_a \otimes \hat{S}(r_b)|0\rangle_b$

With the coherent state and the squeezed vacuum state as inputs, the phase sensitivity at $\phi = 0$ is given by

$$\Delta\phi = \sqrt{\frac{4(1+4N_a\cos^2\theta_a)(\cosh 2r_2+\cos\phi_2\sinh 2r_2)}{\sinh^2 2g(1+4N_a\cos^2\theta_a+\cosh 2r_2+\cos\phi_2\sinh 2r_2)^2}}. \tag{13}$$

Under the condition $\phi_2 = \pi$ and $\theta_a = \pi$, the optimal phase sensitivity is achieved

$$\Delta\phi_{\text{opt}} = \sqrt{\frac{1+4N_a}{\kappa(\cosh r+2N_a\cosh r+2N_a\sinh r)^2}}. \tag{14}$$

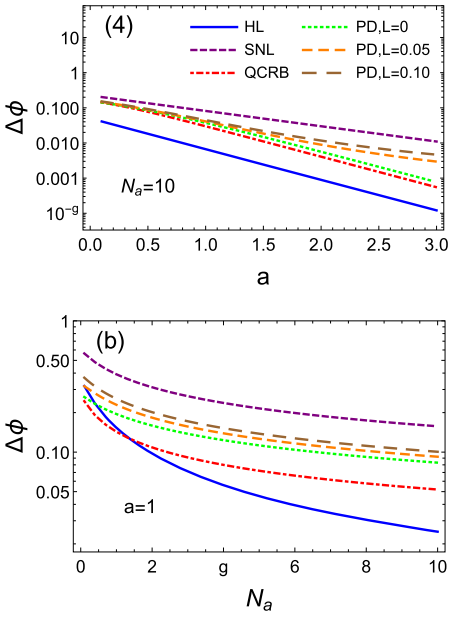

Figure 4 (Color online) Optimal phase sensitivity via product detection as a function of (**a**) g and (**b**) N_a with two coherent input states. The blue line represents the HL, the dashed purple line represents the shot noise limit (SNL), the dot-dashed red line represents the quantum Cramér–Rao bound (QCRB), the dotted green line represents the phase sensitivity via product detection in the ideal case, the dashed red line represents the phase sensitivity via product detection with photon loss $L = 0.05$, and the dashed brown line represents the phase sensitivity via product detection with photon loss $L = 0.10$

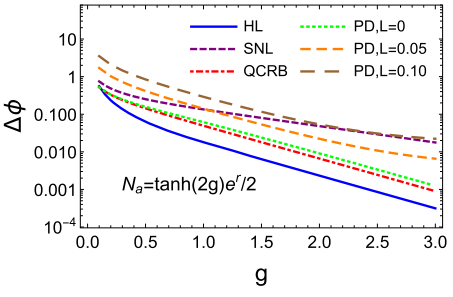

Figure 5 (Color online) Optimal phase sensitivity via product detection as a function of g with the coherent state mixed with the squeezed vacuum state. The blue line represents the HL, the dashed purple line represents the shot noise limit (SNL), the dot-dashed red line represents the quantum Cramér–Rao bound (QCRB), the dotted green line represents the phase sensitivity via product detection in the ideal case, the dashed red line represents the phase sensitivity via product detection with photon loss $L = 0.05$, and the dashed brown line represents the phase sensitivity via product detection with photon loss $L = 0.10$. The parameter values are as follows: $r = 2$, $|\alpha| \simeq \tanh(2g)e^r/2$

We assume that $N_a \gg 1$ and denote r_2 by r, the optimal phase sensitivity is reduced to $1/[\kappa(N_a e^{2r} + \cosh re^r)]^{1/2}$. This result is similar to parity detection [42]. The corresponding HL is $1/[(N_{\rm PA}+1)(N_a+N_s)+N_{\rm PA}]$, where $N_s = \sinh^2 r$. Meanwhile, the QCRB is given by $1/[2N_a(N_{\rm PA}+2)+N_{\rm PA}^2\sinh^2(2r)/2+\kappa(2N_a\cosh re^r+\cosh^2 r)]^{1/2}$. As pointed out in Ref. [42], when $|\alpha| \simeq \tanh(2g)e^r/2$, the phase sensitivity can approach the HL. We plot the phase sensitivity $\Delta\phi_{\rm opt}$ as a function of the interaction strength g in Fig. 5. The phase sensitivity is always below the SNL and close to the HL.

2.2.5 *Two squeezed vacuum states* $\hat{S}(r_a)|0\rangle_a \otimes \hat{S}(r_b)|0\rangle_b$

For simplicity, we consider the case in which $r_1 = r_2 = r$. When $\phi_1 = \phi_2 = 0$ or π, the optimal phase sensitivity at $\phi = 0$ is achieved

$$\Delta\phi_{\rm opt} = \frac{1}{\sqrt{\kappa(2N_s+1)}}. \tag{15}$$

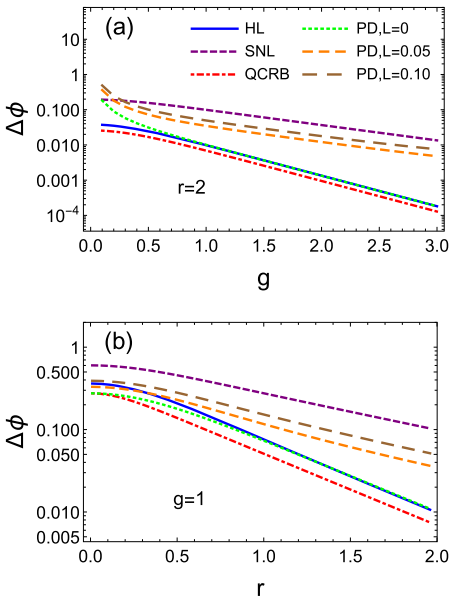

Figure 6 (Color online) Optimal phase sensitivity via product detection as a function of (**a**) g and (**b**) r with two squeezed vacuum states. The blue line represents the HL, the dashed purple line represents the shot noise limit (SNL), the dot-dashed red line represents the quantum Cramér–Rao bound (QCRB), the dotted green line represents the phase sensitivity via product detection in the ideal case, the dashed red line represents the phase sensitivity via product detection with photon loss $L = 0.05$, and the dashed brown line represents the phase sensitivity via product detection with photon loss $L = 0.10$

The corresponding HL is $1/[2(N_{\mathrm{PA}} + 1)N_s + N_{\mathrm{PA}}]$. The QCRB is $1/[(1 + N_{\mathrm{PA}})^2 \cosh 4r - 1]^{1/2}$. The optimal phase sensitivity depends not only on the strength g, but also on the squeezing parameter r, as shown in Fig. 6(a) and (b). Figure 6(a) shows that the phase sensitivity with product detection cannot approach the HL as g increases, while it can easily go below the SNL. When r decreases to zero, phase sensitivity goes back to the case with vacuum inputs, as shown in Fig. 6(b). When r goes to infinity, phase sensitivity would follow the SNL scaling (not shown in Fig. 6). The phase sensitivity is improved by a factor of $1/\sqrt{\cosh 2r}$ compared to the case of vacuum inputs, which comes from noise reduction of the squeezed vacuum states. In this case, the phase sensitivity cannot saturate the QCRB.

3 Discussion

3.1 Comparison between various detections

We have studied the behavior of the phase sensitivity of an SU(1, 1) interferometer with various input states via product detection. Table 1 summarizes the phase sensitivity for different input states with product detection, parity detection and homodyne detection. It also shows the QCRB for different input states.

With vacuum states as inputs, product detection, parity detection and intensity detection all can saturate the QCRB. However, homodyne detection is not available in this case, because the expectation value of the amplitude quadrature operator is always zero, which is independent of phase shift ϕ. From the viewpoint of experimental implementation, intensity detection is greatly preferred because of its simplicity.

In the case with one coherent state as the input (see Fig. 7(a)), product detection achieved the same phase sensitivity as parity detection, and it was slightly better than homodyne detection and intensity detection. All four detection schemes cannot saturate the QCRB. Furthermore, when N_a becomes larger than one, all four detections show the characterization of the SNL scaling, except they included an improvement factor of $1/\sqrt{\kappa}$, which comes from the amplification of the parametric process. When the input photon

Table 1 Phase sensitivities with various detections and QCRB of an SU(1, 1) interferometer with different input states

Input states	Product	Intensity	Parity	Homodyne	QCRB
$\|0\rangle \otimes \|0\rangle$	$1/\kappa^{1/2}$	$1/\kappa^{1/2}$	$1/\kappa^{1/2}$	Not available [42]	$1/\kappa^{1/2}$
$\|\alpha\rangle \otimes \|0\rangle$	$1/[\kappa(N_a+1)]^{1/2}$	$\Delta\phi^{\mathrm{I}}_{\mathrm{onecoh}}$ *	$1/[\kappa(N_a+1)]^{1/2}$	$1/(\kappa N_a)^{1/2}$	$1/[\kappa(2N_a+1)+2N_a(N_{\mathrm{PA}}+2)]^{1/2}$
$\|\alpha e^{i\eta_1}\rangle \otimes \|\alpha e^{i\eta_2}\rangle$ †	$1/\{2N_a[(N_{\mathrm{PA}}+2)(\sqrt{\kappa}+1)+\kappa]+\kappa\}^{1/2}$	$1/(2\kappa N_a)^{1/2}$	Ref. [42]	$\simeq 1/[4\kappa N_a]^{1/2}$	$1/\{4N_a[(N_{\mathrm{PA}}+1)\sqrt{\kappa}+\kappa+1]+\kappa\}^{1/2}$
$\|\alpha\rangle \otimes \hat{S}(r)\|0\rangle$	$1/[\kappa(N_a e^{2r}+\cosh re^{r})]^{1/2}$	$\Delta\phi^{\mathrm{I}}_{\mathrm{cohsqz}}$ ‡	$1/[\kappa(N_a e^{2r}+\cosh^2 r)]^{1/2}$	$1/[\kappa N_a e^{2r}]^{1/2}$	$1/[2N_a(N_{\mathrm{PA}}+2)+N_{\mathrm{PA}}^2\sinh^2(2r)/2+\kappa(2N_a\cosh re^{r}+\cosh^2 r)]^{1/2}$
$\hat{S}(r)\|0\rangle \otimes \hat{S}(r)\|0\rangle$	$1/[\kappa(2N_s+1)]^{1/2}$	$\Delta\phi^{\mathrm{I}}_{\mathrm{twosqz}}$ §	$1/[\kappa(2N_s+1)]^{1/2}$	Not available	$1/[(1+N_{\mathrm{PA}})^2\times\cosh 4r-1]^{1/2}$

*See Section Appendix.
†α is set to be real in this line; it is complex elsewhere.
‡See Section Appendix.
§See Section Appendix.

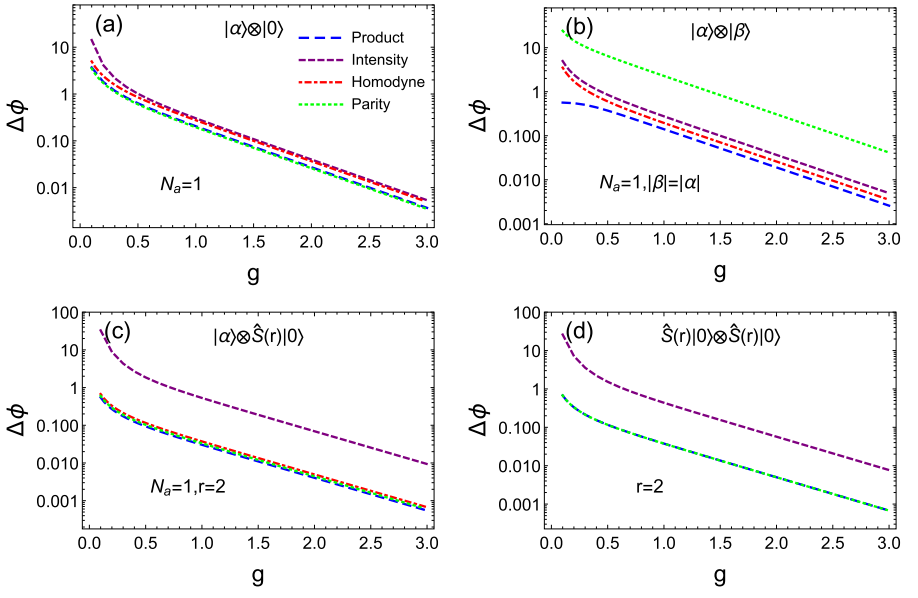

Figure 7 (Color online) Optimal phase sensitivity as a function of g with different detections in the presence of various input states: (**a**) one-coherent state $|\alpha\rangle \otimes |0\rangle$, (**b**) two-coherent state $|\alpha\rangle \otimes |\beta\rangle$, (**c**) coherent and squeezed-vacuum state $|\alpha\rangle \otimes \hat{S}(r)|0\rangle$, (**d**) two-squeezed-vacuum state $\hat{S}(r)|0\rangle \otimes \hat{S}(r)|0\rangle$. The blue line represents the product detection, the dashed purple line represents the intensity detection, the dot-dashed red line represents the homodyne, and the dotted green line represents the parity detection

number is small, product detection is preferred. Otherwise, homodyne detection is the best choice since only one output light beam is measured.

With two coherent states as inputs, the conditions for achieving the optimal phase sensitivity are different as shown in Fig. 7(b). For product detection, the input states is $|\alpha e^{i\pi}\rangle \otimes |\alpha\rangle$. The condition for parity detection and homodyne detection is $|\alpha e^{i\pi/2}\rangle \otimes |\alpha\rangle$, where we assume α is real. From Ref. [42], we know that parity detection is much worse than homodyne detection. On the other hand, product detection can approach the QCRB,

as shown in Fig. 4, and is better than homodyne detection. Therefore, with two coherent states as inputs, product detection is the best scheme. However, all four schemes cannot approach the HL.

To take advantage of the large photon number of the coherent state and the noise reduction of the squeezed vacuum state, coherent states mixed with squeezed vacuum states as inputs have been studied [41, 42]. In this case (see Fig. 7(c)), product detection and parity detection behave similarly. Both schemes can beat the SNL and perform better than homodyne detection. Under the specific condition $|\alpha| \simeq \tanh(2g)e^{r}/2$, the phase sensitivity can approach the HL. Compared to parity detection, product detection is much easier to implement with current homodyne technology. Therefore, it is better to estimate the phase via product detection in this situation.

With both squeezed vacuum states as inputs, the optimal phase sensitivity with product detection and parity detection are the same as depicted in Fig. 7(b). Compared with the case of vacuum states as inputs, it is improved by a factor $1/\sqrt{\cosh 2r}$ as a result of the noise reduction of the squeezed vacuum states.

In general, product detection behaves similarly to parity detection. With both coherent states as inputs, product detection performs better than parity detection. Moreover, it does not require a photon-number resolving detector, which makes it much more feasible than parity detection. It can be easily realized with current homodyne technology.

From Figs. 2, 3, 4, 5, and 6, it is easy to find that the HL can be either above or below the QCRB. In fact, these results are not contradictory. Because HL and QCRB are obtained from different aspects. HL is related to the total mean photon number inside the interferometer while QCRB is dependent on quantum estimation theory which sets the ultimate limit for a set of probabilities that originated from measurements on a quantum system and gives a detection-independent phase sensitivity. For any detection (e.g. intensity detection, homodyne detection, parity detection), the corresponding phase sensitivity is not able to beat the QCRB, but it may reach below the HL.

3.2 Effect of photon loss on the phase sensitivity with product detection

In optical experiment, photon loss is inevitable. Therefore, it is necessary to investigate the effect of photon loss on the performance of an SU(1, 1) interferometer with product detection. Particularly, we concentrate mainly on the photon loss of modes a_1 and b_1 inside the interferometer. Consider modes a_1 and b_1 experience photon loss L_1 and L_2, respectively. For simplicity, we assume that $L_1 = L_2 = L$. Under this situation, one can obtain

$$\begin{aligned}\hat{a}_1^{\text{loss}} &= \sqrt{1-L}\hat{a}_1 + \sqrt{L}\hat{a}_1^{\text{V}},\\ \hat{b}_1^{\text{loss}} &= \sqrt{1-L}\hat{b}_1 + \sqrt{L}\hat{b}_1^{\text{V}},\end{aligned} \tag{16}$$

where $\hat{a}_1^{\text{loss}}$ ($\hat{b}_1^{\text{loss}}$) is the annihilation operator of the mode a (b) after experiencing photon loss, $\hat{a}_1^{\text{V}}$ and $\hat{b}_1^{\text{V}}$ are the annihilation operators corresponding to the vacuum states.

Combining Eqs. (1), (2), (3), (4), and (16), one can obtain the phase sensitivity via product detection with photon loss. To compare between the ideal and the loss situations, we plot the phase sensitivities via product detection with photon loss $L = 0.05$ and $L = 0.10$ in Figs. 2, 3, 4, 5, 6, and 7, respectively. It is easily found that photon loss degrades the phase sensitivity via product detection. Nevertheless, with a small loss, the phase sensitivity via product detection is still able to reach below the SNL in some case.

3.3 Comparison with the previous works

Although both the previous researches [25–29] and our work consider the performance of quantum interferometer, there still is significant difference between them. First of all, unlike these previous papers mainly involving the QCRB, the intensity detection, or the homodyne detection, our work concentrates on the product detection which is still missing in an SU(1, 1) interferometer. Secondly, we compare product detection with other three detections (intensity, parity, homodyne). We present which detection strategy can lead to the better sensitivity in the presence of different state inputs. It is found that product detection is the optimal detection scheme with two-equal-coherent-state input. From this point of view, our results make sense for the optimal choice of meansurement scheme in phase estimation.

4 Conclusion

In summary, we investigated the product detection on an SU(1, 1) interferometer with pure Gaussian states as inputs. We have shown that product detection can approach the HL when the coherent beam and squeezed vacuum beam have roughly equal photon numbers. Compared to parity detection, product detection has a slightly better optimal phase sensitivity with two coherent states as the input, and has the same or a similar phase sensitivity as those of the other four inputs. Product detection always has better phase sensitivity than homodyne detection when non-vacuum states are seeded. We also show the QCRB with various input states. It is difficult for the QCRB to be saturated with product and parity detection and with homodyne detection when non-vacuum states are seeded. The search for the optimal scheme that can saturate the QCRB continues.

Appendix

A.1 Phase sensitivity $\Delta\phi^{\mathrm{I}}_{\mathrm{onecoh}}$

Phase sensitivity with intensity detection with one-coherent-state input is given by

$$\begin{aligned}\Delta\phi^{\mathrm{I}}_{\mathrm{onecoh}} = {}& \big[\operatorname{csch}^4(2g)\big(\sec^2(\phi/2)\big((2N_a+1)\cosh(8g)-1\big)+2N_a\csc^2(\phi/2)\big)\\ & -8(2N_a+1)\big]^{1/2}\big[2\sqrt{2}(N_a+1)\big]^{-1}.\end{aligned} \tag{17}$$

The corresponding optimal phase is found to be

$$\begin{aligned}\phi^{\mathrm{I}}_{\mathrm{onecoh,opt}} = {}& -2\arctan\Big\{\big[\operatorname{csch}^2(4g)\big(\sqrt{2N_a\big((2N_a+1)\cosh(8g)-1\big)}-2N_a\big)\big]^{1/2}\\ & \times(4N_a+2)^{-1/2}\Big\}.\end{aligned} \tag{18}$$

A.2 Phase sensitivity $\Delta\phi^{\mathrm{I}}_{\mathrm{cohsqz}}$

Phase sensitivity with intensity detection with coherent and squeezed-vacuum state input is given by

$$\begin{aligned}\Delta\phi^{\mathrm{I}}_{\mathrm{cohsqz}} = -\big\{ & \operatorname{sech}^4 g\csc^2\phi\big(32\big(\cosh g+\cosh(3g)\big)^2\operatorname{csch}^2 g\cos\phi\big(4e^{-2r}N_a+\cosh(4r)\\ & -1\big)-8\coth^2 g\cos(2\phi)\big(4\sinh^2(2g)\big(4N_a\cosh(2r)+\cosh(4r)-1\big)\\ & -8N_a\big(\cosh(4g)+3\big)\sinh(2r)\big)-64N_a\big(3\cosh(4g)+5\big)\coth^2 g\cosh(2r)\end{aligned}$$

$$+ 64N_a\big(3\cosh(4g) + 1\big)\coth^2 g\sinh(2r) - 2\big(4\cosh(4g) + 3\cosh(8g) + 9\big)$$
$$\times \operatorname{csch}^4 g\sinh^2(2r))\big\}^{1/2}\big\{16\big(2N_a + \cosh(2r)\big)\big\}^{-1}. \tag{19}$$

A.3 Phase sensitivity $\Delta\phi^{\mathrm{I}}_{\mathbf{twosqz}}$

Phase sensitivity with intensity detection with two-squeezed-vacuum state input is given by

$$\Delta\phi^{\mathrm{I}}_{\mathrm{twosqz}} = \frac{1}{2\sqrt{2}}\operatorname{csch}(2g)\operatorname{sech}(2r)\big(\operatorname{csch}^2(2g)\big(\sec^2(\phi/2)\big(\cosh(8g)\cosh(4r) - 1\big)$$
$$+ 2\sinh^2(2r)\csc^2(\phi/2)\big) - 4\cosh(4g)\cosh(4r) + 4\big)^{1/2}. \tag{20}$$

The corresponding optimal phase is found to be

$$\phi^{\mathrm{I}}_{\mathrm{twosqz,opt}} = 2\arctan\Big\{\Big[\operatorname{csch}^2(4g)\Big(\operatorname{sech}(4r)\Big(\sqrt{2\sinh^2(2r)\big(\cosh(8g)\cosh(4r) - 2\big)}$$
$$+ 1\Big) - 1\Big)\Big]^{1/2}/\sqrt{2}\Big\}. \tag{21}$$

Acknowledgements
Yami Fang would like to acknowledge support from Fudan University postdoctoral research program.

Funding
This work was supported by NSFC (Grant No. 61801126), Open project of CAS Key Laboratory of Quantum Information, University of Science and Technology of China (Grant No. KQI201902), Beijing municipal organization department youth backbone talent project (Grant No. 201800002685XG356), the Fundamental Research Funds for the Central Universities (Grant No. 2020MS014).

Abbreviations
SNL, shot noise limit; HL, Heisenberg limit; BECs, Bose–Einstein condenstates; QCRB, quantum Cramér–Rao bound.

Availability of data and materials
Not applicable

Competing interests
The authors declare that they have no competing interests.

Authors' contributions
QW implemented numerical simulations and was a major contributor in writing the manuscript. YF contributed to the initiation of the research. XM contributed to writing and revising the manuscript. DL contributed to the comment and revision of the manuscript. All authors read and approved the final manuscript.

Author details
[1]School of Control and Computer Engineering, North China Electric Power University, 102206 Beijing, China. [2]CAS Key Laboratory of Quantum Information, University of Science and Technology of China, 230026 Hefei, China. [3]Shanghai Aerospace Control Technology Institute, 201109 Shanghai, China. [4]Shanghai Key Laboratory of Aerospace Intelligent Control Technology, 201109 Shanghai, China. [5]College of Mathematical and Physical sciences, Qingdao University of Science and Technology, Songling Road 99, 266061 Qingdao, China. [6]Microsystems and Terahertz Research Center, China Academy of Engineering Physics, 610200 Chengdu, China. [7]Institute of Electronic Engineering, China Academy of Engineering Physics, 621999 Mianyang, China.

Publisher's Note

Received: 13 December 2020 Accepted: 2 August 2021 Published online: 17 August 2021

References

1. Helstrom CW. Quantum detection and estimation theory. New York: Academic Press; 1976.
2. Giovannetti V, Lloyd S, Maccone L. Science. 2004;306:1330.

3. Demkowicz-Dobrzański R, Jarzyna M, Kolodyński J. Prog Opt. 2015;60:345.
4. Hosten O, Krishnakumar R, Engelsen NJ, Kasevich MA. Science. 2016;352:1552.
5. Hosten O, Engelsen NJ, Krishnakumar R, Kasevich MA. Nature. 2016;529:505.
6. Gao Y. Phys Rev A. 2016;94:023834.
7. Chekhova MV, Ou ZY. Adv Opt Photonics. 2016;8:104.
8. Szczykulska M, Baumgratz T, Datta A. Adv Phys X. 2016;1:621.
9. Abbott BP, Abbott R, Abbott TD et al. Phys Rev Lett. 2016;116:131103.
10. Lee H, Kok P, Dowling JP. J Mod Opt. 2002;49:2325.
11. Ou ZY. Phys Rev A. 2012;85:023815.
12. Lang MD, Caves CM. Phys Rev Lett. 2013;111:173601.
13. Giovannetti V, Lloyd S, Maccone L. Phys Rev Lett. 2006;96:010401.
14. Pezzé L, Smerzi A. Phys Rev Lett. 2009;102:100401.
15. Caves CM. Phys Rev D. 1981;23:1693.
16. Bondurant RS, Shapiro JH. Phys Rev D. 1984;30:2548.
17. Steuernagel O, Scheel S. J Opt B, Quantum Semiclass Opt. 2004;6:S66.
18. Holland MJ, Burnett K. Phys Rev Lett. 1993;71:1355.
19. Bollinger JJ, Itano WM, Wineland DJ, Heinzen DJ. Phys Rev A. 1996;54:R4649.
20. Lee H, Kok P, Dowling JP. J Mod Opt. 2002;49:2325.
21. Dowling JP. Contemp Phys. 2008;49:125.
22. Yurke B, McCall SL, Klauder JR. Phys Rev A. 1986;33:4033.
23. Plick WN, Dowling JP, Agarwal GS. New J Phys. 2010;12:083014.
24. Marino AM, CorzoTrejo NV, Lett PD. Phys Rev A. 2012;86:023844.
25. Sparaciari C, Olivares S, Paris MGA. J Opt Soc Am B. 2015;32(7):1354–9.
26. Sparaciari C, Olivares S, Paris MGA. Phys Rev A. 2016;93:023810.
27. Hu X-L, Li D, Chen LQ, Zhang K, Zhang W, Yuan C-H. Phys Rev A. 2018;98:023803.
28. You CL, Adhikari S, Ma XP, Sasaki M, Takeoka M, Dowling JP. Phys Rev A. 2019;99:042122.
29. Zheng KM, Mi MH, Wang B, Xu L, Hu LY, Liu SS, Lou YB, Jing JT, Zhang LJ. Photonics Res. 2020;8:1653–61.
30. Jing J, Liu C, Zhou Z, Ou ZY, Zhang W. Appl Phys Lett. 2011;99:011110.
31. Hudelist F, Kong J, Liu C, Jing J, Ou ZY, Zhang W. Nat Commun. 2014;5:3049.
32. Linnemann D. Realization of an SU(1, 1) interferometer with spinor Bose–Einstein condensates [Master thesis]. 2013.
33. Linnemann D, Strobel H, Muessel W, Schulz J, Lewis-Swan RJ, Kheruntsyan KV, Oberthaler MK. Phys Rev Lett. 2016;117:013001.
34. Gross C, Zibold T, Nicklas E, Estève J, Oberthaler MK. Nature. 2010;464:1165.
35. Peise J, Lücke B, Pezzé L, Deuretzbacher F, Ertmer W, Arlt J, Smerzi A, Santos L, Klempt C. Nat Commun. 2015;6:6811.
36. Gabbrielli M, Pezzè L, Smerzi A. Phys Rev Lett. 2015;115:163002.
37. Chen B, Qiu C, Chen S, Guo J, Chen LQ, Ou ZY, Zhang W. Phys Rev Lett. 2015;115:043602.
38. Chen ZD, Yuan C-H, Ma HM, Li D, Chen LQ, Ou ZY, Zhang W. Opt Express. 2016;24:17766.
39. Barzanjeh Sh, DiVincenzo DP, Terhal BM. Phys Rev B. 2014;90:134515.
40. Szigeti SS, Lewis-Swan RJ, Haine SA. Phys Rev Lett. 2017;118:150401.
41. Li D, Yuan C-H, Ou ZY, Zhang W. New J Phys. 2014;16:073020.
42. Li D, Gard BT, Gao Y, Yuan C-H, Zhang W, Lee H, Dowling JP. Phys Rev A. 2016;94:063840.
43. Hu XY, Wei CP, Yu YF, Zhang ZM. Front Phys. 2016;11:114203.
44. Braunstein SL, Caves CM. Phys Rev Lett. 1994;72:3439.
45. McCormick CF, Marino AM, Boyer V, Lett PD. Phys Rev A. 2008;78:043816.
46. Fang Y, Jing J. New J Phys. 2015;17:023027.
47. Gao Y, Lee H. Eur Phys J D. 2014;68:347.